JOURNAL OF MATERIALS SCIENCE 24 (1989) 2687–2696

Shear yielding modes of polycarbonate

M. MA*, K. VIJAYAN†, A. HILTNER and E. BAER
Center for Applied Polymer Research, and Department of Macromolecular Science, Case Western Reserve University, Cleveland, Ohio 44106, USA

J. IM
The Dow Chemical Company, Midland, Michigan 48640, USA

The modes of shear yielding in edge-notched sheets of polycarbonate have been studied under slow tensile loading. Optical microscope techniques were used to characterize the flow lines through the thickness of the plastically deformed region. Three modes are observed, namely core yielding, hinge shear and intersecting shear. Core yielding consists of two families of shear flow lines contained in the centre region where the stress is highest. In the nearly plane strain condition, the dominating shear mode is hinge shear which is through-thickness yielding on inclined planes above and below the notch. Intersecting shear dominates in the nearly plane stress condition. In this case, yielding occurs through the entire thickness by slip along planes parallel to the width direction that make an angle with the plane of the sheet. It produces a necking effect in front of the notch. The thickness dependent transition from hinge shear to intersecting shear follows conditions suggested by Hahn and Rosenfield.

1. Introduction

Polycarbonate is a tough, ductile material which deforms by shear yielding even at cryogenic temperatures [1]. However, typical of a ductile thermoplastic, it is extremely notch sensitive. Embrittlement of polycarbonate is also dependent on specimen thickness, molecular weight, thermal history, strain rate and test temperature. Hence, the failure of polycarbonate depends on a number of complex interacting phenomena, not all of which are completely understood.

The importance of the plastic deformation zone in polycarbonate has been widely recognized. Mills [2], Kitagawa [3], and Ishikawa *et al.* [4] have described a plastic zone which resembles the slip line field emanating from a circular notch when they tested thick specimens undergoing plane strain deformation. In thinner specimens, Nisitani and Hyakutake [5] observed a similar zone which was accompanied at higher strains by large surface shear bands. This mode was characteristic of blunt notches only, for more sharply notched specimens failed in an apparently brittle manner. The type of damage zone created by the large surface shear bands was also observed by Haddaoui *et al.* [6] when even thinner specimens with a blunt notch were tested under cyclic fatigue. They associated it with a thinning or necking phenomenon. The so-called epsilon plastic zone has been observed during discontinuous fatigue crack growth in un-notched polycarbonate [7–9]. This zone consists of a leading craze and a pair of sharply delineated shear bands that develop during the multiple load cycles between crack jumps.

Under sharp notch conditions that produced a relatively small damage zone, on the size scale of the crack, polycarbonate was reported to obey the Dugdale model of ductile yielding [10]. However, for blunt notches that result in large amounts of plastic yielding, the Dugdale model becomes invalid. Instead, plasticity theory could be used, which describes the instability due to large plastic flow in rigid plastic materials and has found wide application to ductile metals. Specifically, it provides a vehicle for understanding the relationship of the stress state, as determined by thickness, notch geometry, applied stress, etc., to the shear yielding mode. This study first addresses characterization of the various shear yielding modes in polycarbonate, and then identification of relationships among the various modes in terms of analytical concepts of plasticity theory.

2. Experimental procedure

Polycarbonate (PC) samples were provided by The Dow Chemical Company, Freeport, Texas. Calibre (Trademark, The Dow Chemical Company) 22 was supplied in the form of 3 in. × 2 in. (~7.62 cm × 5.08 cm) injection-moulded plaques with thicknesses of 3.14 mm, 4.70 mm and 6.54 mm. Merlon (Trademark, Mobay Chemical Corporation, Pittsburgh, Pennsylvania) M-40 was supplied in the form of 1.20 mm thick extruded sheet. Rectangular specimens 20 mm wide were single-edge notched and mounted in an Instron testing machine with a length of 60 mm between the grips. For the 6.54 mm thickness only, single-edge notched specimens with a dumb-bell-shaped geometry were used in order to obtain sufficient

* *Present address*: Rogers Corporation, Rogers, Connecticut 06263, USA.
† *Present address*: Richards Medical Company, Memphis, Tennessee 38116, USA.

0022–2461/89 $03.00 + .12

gripping during testing. The gauge section in this case was 20 mm wide and 25 mm long. For convenience, the loading direction is identified as the z-direction, and the width and thickness as the x- and y-directions, respectively.

Various notch geometries were used. The semicircular notch was machined with a 1 mm radius. The 60° and 30° blunt notches were 1 mm in depth with a notch radius of 2.5 μm. Sharp notches were achieved by pressing a razor blade slowly to a depth of 1 mm. Tensile tests were carried out at room temperature with a cross-head speed of 0.1 mm min^{-1}. At least five specimens were tested and a typical stress–displacement curve is reported. A travelling optical microscope with a 35 mm camera was used to photograph the yield zone at 0.1 mm intervals during extension.

To obtain sections of the yield zone, a specimen was loaded to the desired point on the stress–displacement curve, carefully unloaded and trimmed with a bandsaw. The specimen was then ground to the desired depth on a polishing wheel with fine sandpaper, polished with a 50% suspension of 1.0 μm aluminium oxide powder from the Buehler Company, and viewed in an Olympus Model SZH stereo optical microscope in transmission under polarized light.

3. Results

3.1. Hinge shear mode in thick sheet

The stress–displacement curve of the 6.54 mm thick polycarbonate with a semicircular notch is shown in Fig. 1. The specimen was photographed during deformation, and the arrows indicate the positions at which the following sequence of micrographs was taken. The micrographs are from the nonlinear region and show macroscopic shear yielding prior to crack initiation and growth. Yielding occurs first in the centre of the specimen at the notch tip where the stress is a maximum in plane strain tension. Core yielding is observed in Fig. 2a which corresponds to position 1 in Fig. 1 Although the slip lines cannot be clearly distinguished in Fig. 2a because the focus is on the surface, the two families of curving flow lines that grow out from the notch at an angle of 45° and intersect each other at 90°

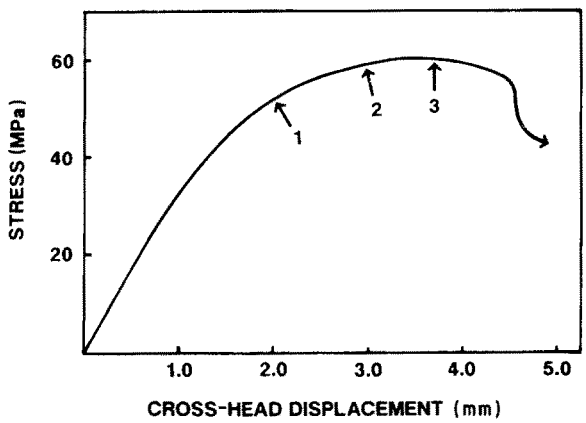

Figure 1 Stress–displacement curve of 6.54 mm thick PC with a semicircular notch. Numbers on the curve indicate positions at which micrographs of the yield zone were obtained.

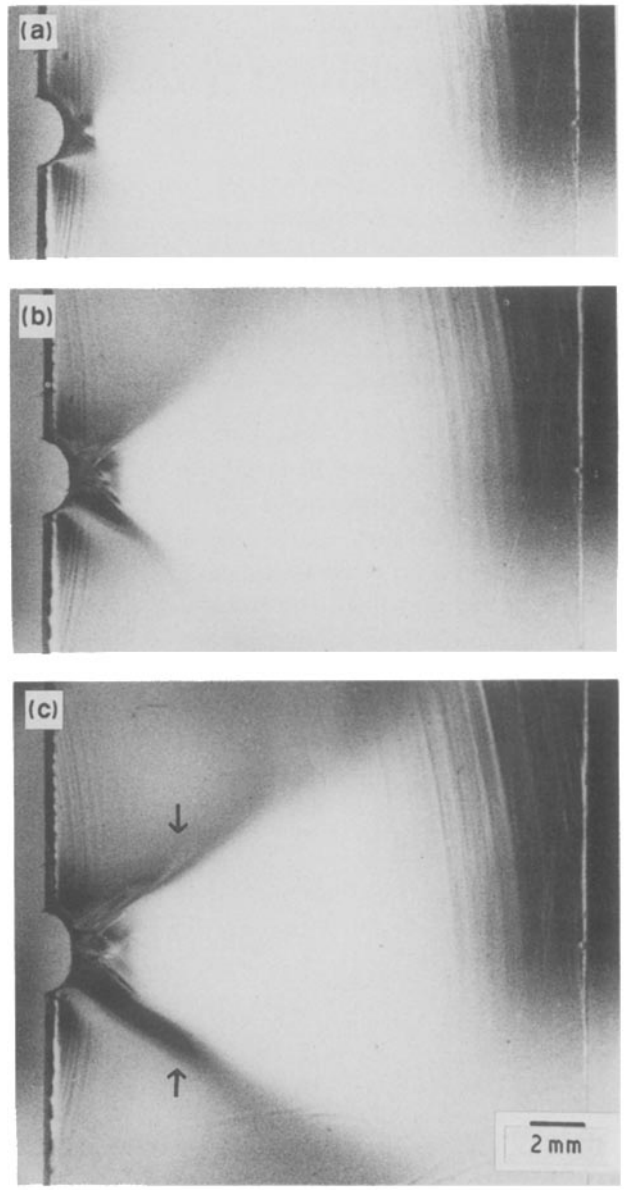

Figure 2 Micrographs showing the yield zone of 6.54 mm thick PC with a semicircular notch at the various positions indicated in Fig. 1. (a) Position 1, (b) position 2, and (c) position 3.

will be visible in a subsequent micrograph of a slightly thinner specimen. With increasing stress, the core yielding ceases to grow and a second shear mode, hinge shear, appears as two dark bands that extend from the notch above and below the core yielding at an angle of 40° to the x-direction, Fig. 2b. The hinge shear bands lengthen across the width as the stress increases, Fig. 2c; specimens of this thickness fracture through one of the hinge shear bands after the hinges reach the opposite edge.

A specimen was loaded a little beyond position 3 and the damage zone sectioned at the position of the arrows in Fig. 2c. Fig. 3 shows the polished section as viewed in the polarizing optical microscope. Below the plane of focus, the notch appears as a dark horizontal zone. Above and below the notch where the section would cut through the hinge shear bands, birefringent isostrain fringes extend horizontally through the specimen indicating that this mode of yielding is

Figure 3 (Opposite) Polarized light micrograph of the yield zone of 6.54 mm thick PC near position 3 sectioned at the position of the arrows in Fig. 2c and viewed in the yz plane.

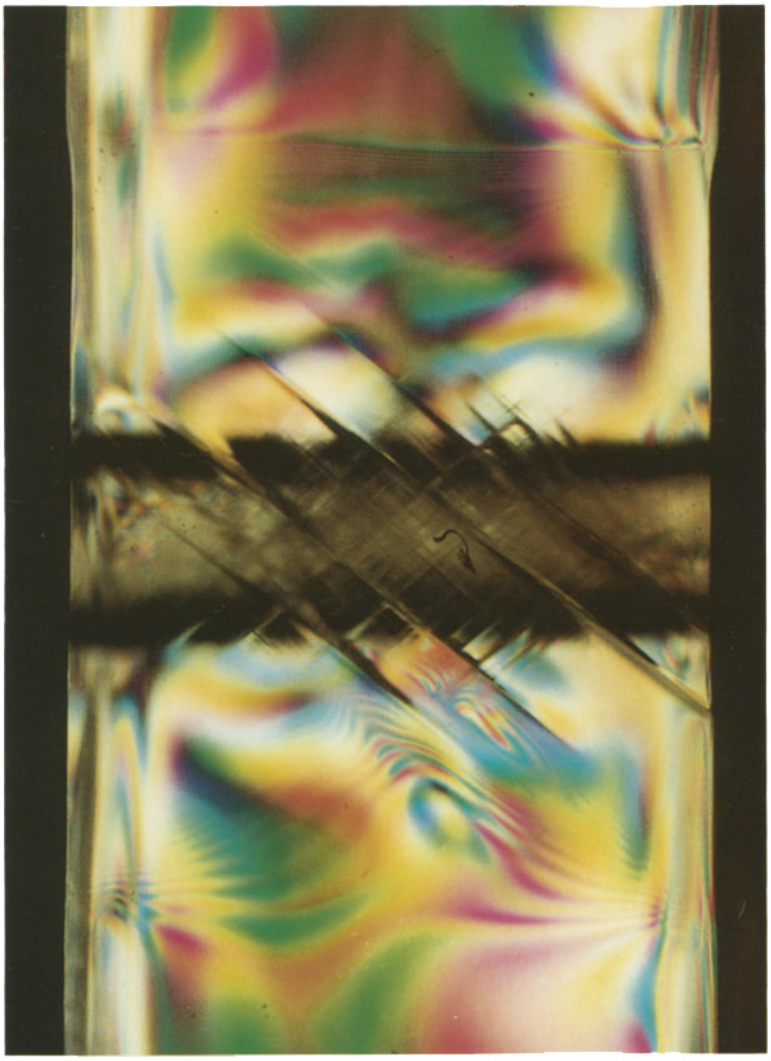

1 mm

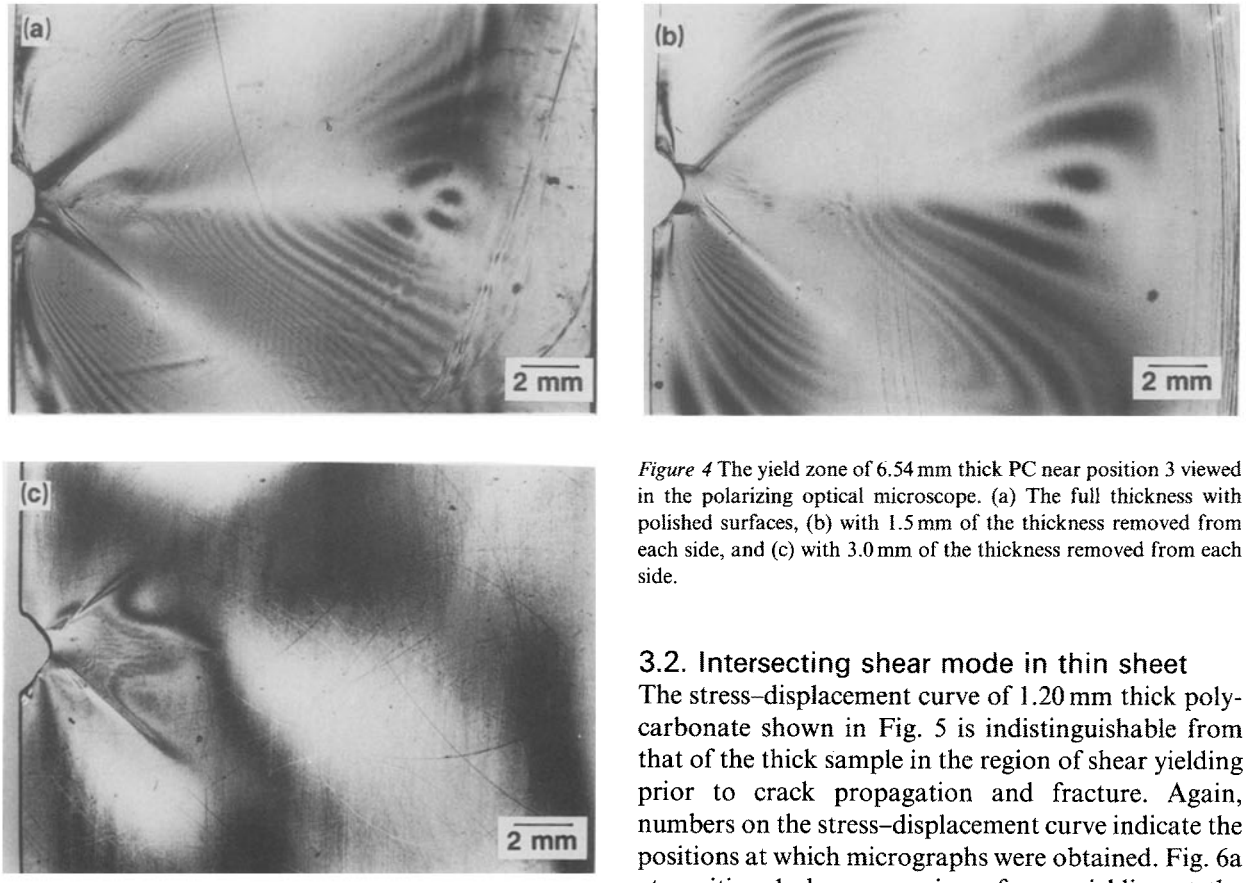

Figure 4 The yield zone of 6.54 mm thick PC near position 3 viewed in the polarizing optical microscope. (a) The full thickness with polished surfaces, (b) with 1.5 mm of the thickness removed from each side, and (c) with 3.0 mm of the thickness removed from each side.

through the thickness. A slight change in the surface contour caused by the localized shear displacement is clearly evident where the hinge shear intersects the surface. Light scattering from this surface curvature produces the dark bands when hinge shear is viewed as in Fig. 2 with unpolarized light. The 45° slip lines in the centre region derive from the core yielding.

That hinge shear is through-thickness yielding is also demonstrated with a 6.54 mm specimen loaded to position 3 and subsequently reduced in the thickness direction. Increments of about 0.5 mm were removed from each surface, the surfaces were polished and the section examined in the polarizing optical microscope until only about 0.5 mm from the centre of the specimen remained. A view of the entire thickness with the surfaces polished, Fig. 4a, shows the flow lines of hinge shear at the centre of two lobes of birefringent isostrain contours. The flow lines remain visible when 1.5 and 3.0 mm are removed from each surface of the specimen, Fig. 4b and c; they extend from the notch at a constant angle of 40° to a length that decreases only slightly from the surface to the core. The birefringent contours in the 0.5 mm section of the centre, Fig. 4c, also reveal the core yielding zone. The distortion of the notch profile in this section is caused by core yielding. The polarized micrographs give a direct view of the flow lines while the dark bands in the unpolarized micrographs of unpolished specimens are caused by light scattering from surface distortions created during hinge shear. Because a comparison shows that the dark bands superimpose the flow lines, the former are used to measure the length and angle of hinge shear bands.

3.2. Intersecting shear mode in thin sheet

The stress–displacement curve of 1.20 mm thick polycarbonate shown in Fig. 5 is indistinguishable from that of the thick sample in the region of shear yielding prior to crack propagation and fracture. Again, numbers on the stress–displacement curve indicate the positions at which micrographs were obtained. Fig. 6a at position 1 shows a region of core yielding at the notch tip; it is smaller than in the thick sheet and without the well-defined characteristic flow lines of the thicker sheets. The dark areas above and below this zone may be the beginning of hinge shear, but rather than further growth of hinge shear bands, a third shear mode, intersecting shear, is observed at position 2, Fig. 6b. Intersecting shear appears as a pair of dark bands that curve away from the notch until the two bands are parallel to each other and perpendicular to the stress direction. With increasing stress, the parallel bands of intersecting shear lengthen across the width of the specimen, Fig. 6c, until the specimen fractures by a slow tearing mode through the centre.

A cross-section of the damage zone, Fig. 7, cut parallel to the stress direction at the position of the arrows in Fig. 6c, shows a pair of broad intersecting

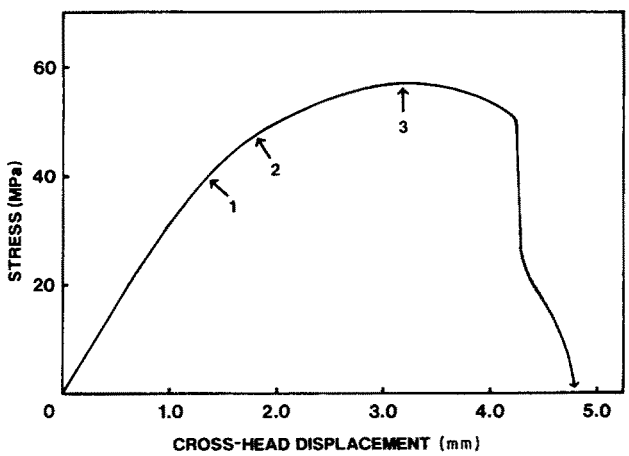

Figure 5 Stress–displacement curve of 1.20 mm thick PC with a semicircular notch. Numbers on the curve indicate positions at which micrographs of the yield zone were obtained.

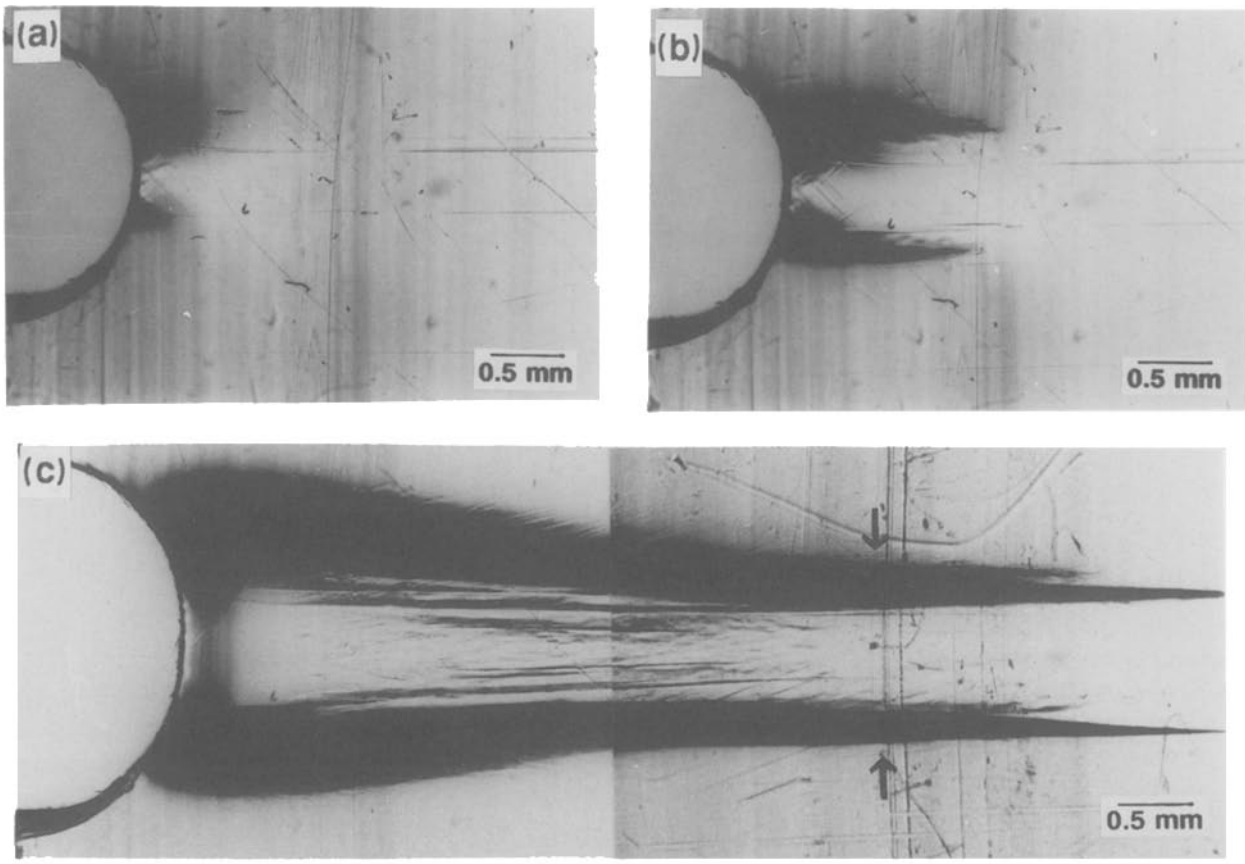

Figure 6 Micrographs showing the yield zone of 1.20 mm thick PC with a semicircular notch at the various positions indicated in Fig. 5. (a) Position 1, (b) position 2, and (c) position 3.

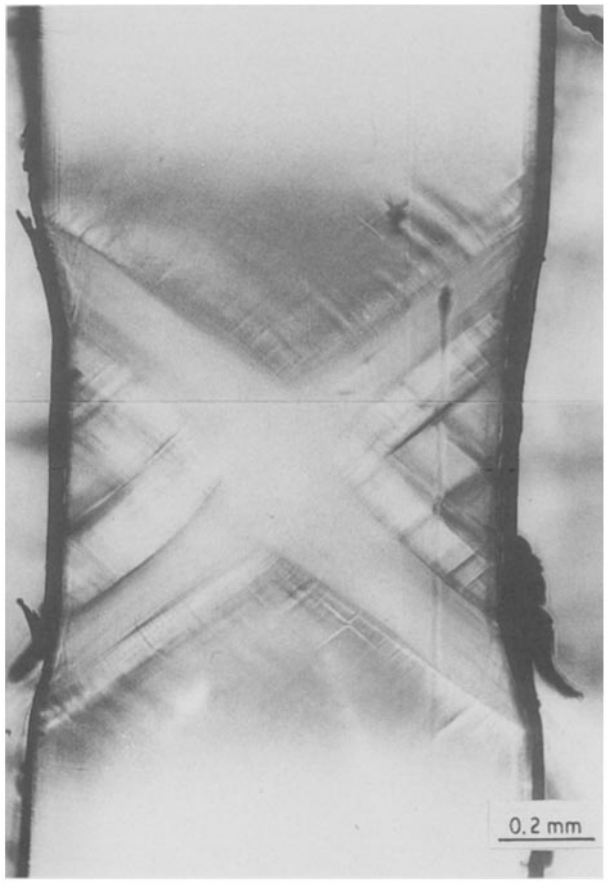

Figure 7 Polarized light micrograph of the yield zone of 1.20 mm thick PC at position 3 sectioned at the position of the arrows in Fig. 6c and viewed in the *yz* plane.

flow lines that extend through the thickness of the specimen at an angle of 53° to the loading direction when viewed in the polarizing optical microscope. Surface curvature caused by localized shear displacement and thinning of the specimen are clearly evident. Light scattering from the surface curvature where the flow lines intersect the surface produces the parallel dark bands that characterize intersecting shear when viewed without polars as in Fig. 6c.

3.3. Multiple shear modes

The stress–displacement curve of 4.70 mm thick polycarbonate with a semicircular notch is shown in Fig. 8

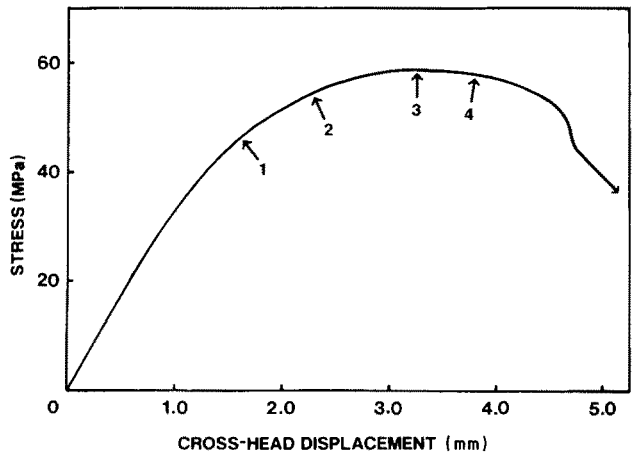

Figure 8 Stress–displacement curve of 4.70 mm thick PC with a semicircular notch. Numbers on the curve indicate positions at which micorgraphs of the yield zone were obtained.

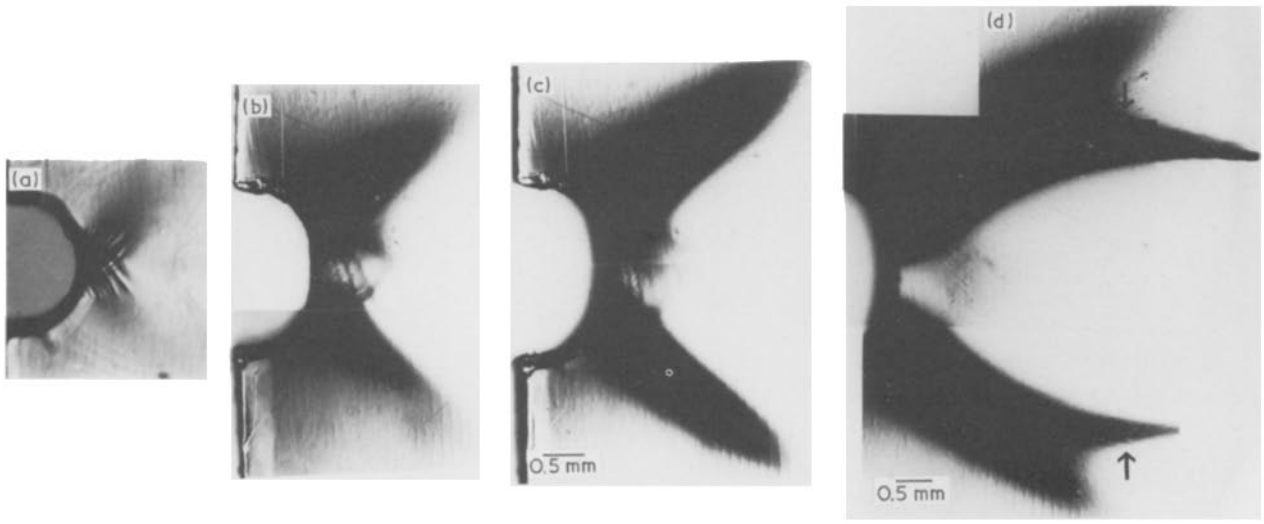

Figure 9 Micrographs showing the yield zone of 4.70 mm thick PC with a semicircular notch at the various positions indicated in Fig. 8. (a) Position 1, unloaded with the focus on the centre of the specimen, (b) position 2, (c) position 3, and (d) position 4.

with the positions indicated at which the specimen was photographed. The first observable shear mode is again core yielding. The specimen shown in Fig. 9a was loaded to position 1, unloaded and the photograph taken with the focus adjusted to the centre of the specimen. The two families of curving flow lines that grow out from the notch tip at an angle of 45° and intersect each other at 90° are clearly defined. In Fig. 9b at position 2 the specimen is under tension and the focus is on the surface. The core yielding is out of focus and partially obscured by the second shear mode, hinge shear, which appears as two dark bands above and below the core yielding. The hinge shear bands extend away from the notch at approximately 40° and continue to lengthen as the stress increases while there is little, if any, growth of the core yielding zone (Fig. 9c). The third shear mode, intersecting shear, appears between positions 3 and 4. A second pair of dark bands in Fig. 9d at position 4 curves away from the notch until the two bands are parallel to each other. After the intersecting shear mode appears, growth of the hinge shear bands slows down and stops while the intersecting shear bands continue to lengthen across the width of the specimen until the specimen fractures through the centre.

Fig. 10 shows a longitudinal cross-section of the damage zone cut at the position of the arrows in Fig. 9d as seen in the polarizing optical microscope. In this micrograph, the focus is on the core yielding zone which is clearly contained in the centre region of the specimen. Because slip lines can also form near the notch surface in the *yz* plane, core yielding appears as numerous orthogonal lines at 45° to the loading direction. These slip lines are much shorter than in Fig. 9a because their origin is not from a curved free surface. Below the plane of focus the notch appears as a dark horizontal zone, and above the plane of focus the broad flow lines of intersecting shear extend through the thickness of the specimen at an angle of 53° to the loading direction.

The stress–displacement curves are indistinguishable for the various thicknesses except for subtle differences in the crack propagation and fracture region. A slightly thinner specimen, 3.14 mm thick, deformed to the equivalent of position 3 in Fig. 8, also shows all three modes including intersecting shear, Fig. 11. In

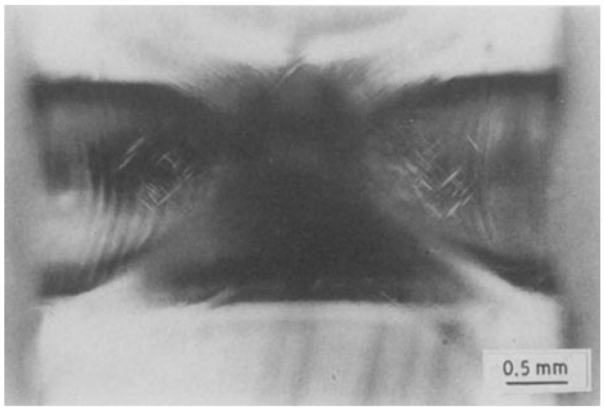

Figure 10 Polarized light micrograph of the yield zone of 4.70 mm thick PC at position 4 sectioned at the position of the arrows in Fig. 9d and viewed in the *yz* plane.

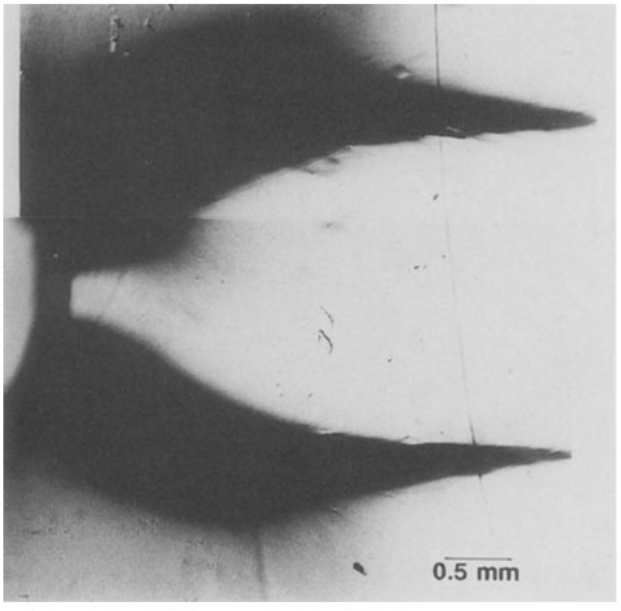

Figure 11 Micrograph showing the yield zone of 3.14 mm thick PC with a semicircular notch near the equivalent of position 3 in Fig. 8.

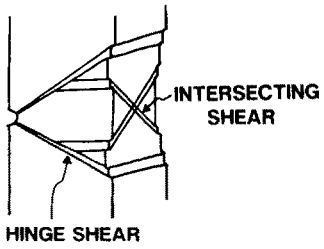

Figure 12 Schematic representation of shear modes observed in PC.

addition to occurring at a lower stress, the parallel bands of intersecting shear are closer together in the 3.14 mm thick sheet than in the 4.70 mm. Because the dark bands in the optical microscope occur where the flow lines intersect the surface, the distance separating the parallel bands depends on the thickness of the specimen and is equal to t cot 53°, where t is the sheet thickness.

The two modes of shear as they occur in the 3.14 and 4.70 mm thick sheet are shown schematically in Fig. 12. Hinge shear extends normal to the plane of the sheet so that its form is essentially the same at all interior sections. Intersecting shear is projected in front of the notch and occurs along planes inclined at 53° to the tensile direction, hence the width of the zone is determined by the thickness of the sheet. Viewed from the side, intersection of the two sets of slip planes with the surface produces the dark bands in Fig. 9d and Fig. 11.

The observed hinge angle is 40° regardless of sheet thickness when the semicircular notch geometry is used, but increases when the notch is made sharper. With a 60° blunt notch the hinge angle increases to 50° while the stress–displacement curve is the same as that of the semicircular notch and fracture occurs at about the same stress. Hinge shear bands were observed with sharper notches in the 4.70 mm sheet but in these cases a crack initiated at the notch root near position 2 on the stress–displacement curve, Fig. 8, and catastrophic fracture followed before the onset of intersecting shear. With a 30° blunt notch the hinge shear bands appear at an angle of 60° and with a razor notch the hinge angle is 70°.

4. Discussion

4.1. Plane strain shear modes

A notched specimen loaded in uniaxial tension experiences the maximum stress at the notch tip; if the sheet is thick enough, the stress cannot be assumed uniform through the thickness but will be triaxial with $\sigma_z > \sigma_y > \sigma_x$ and greatest at the centre. Failure will occur first at this position, but the mechanism by which the stress concentration is relieved depends on the particular material; possible mechanisms include crack initiation leading to fracture, cavitational mechanisms such as crazing, or shear yielding as is observed here with polycarbonate. In considering the failure of a perfectly elastic plastic material in plane strain, various publications [2–4, 11–13], following the suggestions of Hill [14], have described the formation of two sets of shear slip lines, α and β, that emanate from the curved notch surface at 45° respectively above and below the notch tip in a logarithmic spiral

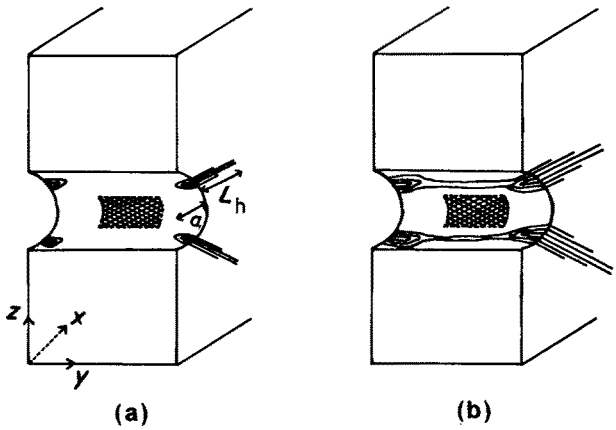

Figure 13 Schematic representation of hinge shear. (a) Initiation at the surface, and (b) growth through the thickness.

such that the two sets intersect at 90°. The slip lines observed experimentally in polycarbonate are characteristic, the angles formed by the intersection of the slip lines with the notch surface and with each other are 45° and 90°, respectively, as predicted. Because the stress state is triaxial near the notch tip, an additional set of α' and β' slip lines can form in the yz plane along the maximum shear directions 45° to the z-axis. These lines, observed experimentally in Fig. 10, for example, can extend only a short distance, however, because they do not originate from a curved free surface.

Plane strain core yielding cannot grow beyond a certain point being kinematically constrained by the surrounding elastic material, but in the external region the surface condition provides a larger degree of freedom for extended yielding. Fig. 13 shows schematically the development of hinge shear following core yielding in a thick sheet with a perspective view of the notch surface. Because there is no constraint in the thickness direction near the surface, hinge shear initiates at four points on the edges of the notch surface, Fig. 13a. The hinge shear grows in length with increasing stress and penetrates the entire thickness, Fig. 13b, so that a pair of hinge shear bands grows out from the notch surface, one above and one below the core yielding zone.

Hinge shear has been observed in metals and ceramic materials by Orowan [15] and others [16, 17] where it was identified with sliding of linear dislocation arrays. Hinge shear together with core yielding had been observed on single-edge notch specimens of silicon steel tested under plane strain conditions [18] and also on Charpy specimens of high nitrogen steel in a three-point flexural mode [19]. Hinge shear probably produces the characteristic epsilon damage zone observed during fatigue fracture of polycarbonate.

The problem of plastic yielding on inclined planes at the tip of a notch in plane strain has been studied by Bilby and Swinden [20] who described the plastic zone by an array of dislocations with Burgers vectors making an angle with the crack. For the situation of plane strain, they made some limited calculations for an angle of 45°. Subsequently, Vitek [21], extending this approach, represented the deformation by a statistical distribution of edge dislocations and obtained approximate analytical expressions as functions of the

applied stress and slip plane angle. A purely analytical approach for plane strain yielding consisting of two slip bands emanating symmetrically from the crack tip of a perfectly elastic plastic solid has been described by Rice [22].

The purely analytical approach of Rice predicts the angle of maximum shear strain at 70.6° for a sharp notch under plane strain conditions. The experimental observations of Hahn and Rosenfield [18] show the hinge at 70° when the zone is small but as larger scale yielding occurs the hinge bands become curved so that the angle is significantly decreased. The hinge bands in the epsilon damage zone of polycarbonate shown by Takemori and Matsumoto [9] and Mills and Walker [7], for example, also curve away from the crack from an initial angle near 70° to an angle of about 40°. The decreasing angle can be attributed to gradual notch blunting, so that the initial angle conforms with the sharp notch condition when the zone is small, but approaches the Tresca condition as the zone grows. Experimentally, the hinge angle in polycarbonate depends on the notch geometry; with a semicircular notch the hinge angle of 40° is closer to the Tresca condition for the unnotched case. When the notch is made sharper, the hinge angle increases to 70° for a razor notch. Curvature in the hinge is not observed, either because the initial notch geometry is already close to the Tresca condition, or, with sharper notches, fracture occurs before hinge growth can proceed very far.

The dependence of hinge shear band length on the applied tensile stress is shown in Fig. 14 for the 60° notch case. For those thicknesses that also exhibit intersecting shear, only data for stresses below the onset of intersecting shear are plotted. For comparison, the predictions of several models are also included. All assume a sharp notch geometry where there would not be core yielding. Because very limited data were obtained before the 30° and sharp notch specimens fractured, it is most appropriate to compare the 60° notch data rather than the semicircular notch data because the core yielding zone is much smaller, although the data for the semicircular notch are similar to those in Fig. 14. Mills and Walker [7] found that the length of shear bands in the epsilon damage zone of fatigued polycarbonate agreed with the relationship used by Vitek [21] for a hinge angle of 65° and fit the equation

$$L_h/a = 0.015 \exp\left[6.642\left(\frac{\sigma}{\sigma_{ys}}\right)\right] \quad (1)$$

where L_h is the hinge length, a the notch length, σ and σ_{ys} the tensile stress and yield stress of PC, respectively. However, using the approach of Bilby, Cottrell and Swinden (BCS) [23], Hahn and Rosenfield [18], following Tetelman [24], described the length of hinge shear in silicon steel by the expression

$$L_h/a = 1/2\left[\sec\left(\frac{\pi\sigma}{2\sigma_{ys}}\right) - 1\right] \quad (2)$$

The present data appear to fit this model the best, as shown in Fig. 14. In the Rice [22] model, the displacement is given by

$$L_h/a = \frac{\pi^2}{16}\sin^2\phi(1 + \cos\phi)\left(\frac{\sigma}{\sigma_{ys}}\right)^2 \quad (3)$$

The slip band angle which gives the maximum shear displacement, $\phi = 70.6°$, was used for the comparison in Fig. 14. Because this approach considers small-scale yielding with a linear elastic fracture mechanics approach, it cannot be expected to describe the data, particularly at large deformation where the yield zone becomes large compared to the notch.

4.2. Plane stress shear mode

If the sheet thickness is small, $\sigma_y = 0$ will be approximately satisfied through the entire thickness; when the stress at the notch reaches the yield stress, yielding will occur through the entire thickness by slip along planes parallel to the x-axis making an angle with the plane of the sheet. This would appear to be the type of damage zone observed by Nisitani and Hyakutake [5] and Haddaoui *et al.* [6] in polycarbonate, and has also been reported in edge-notched silicon steel [18] and cracked steel sheet [25]. While the angle will be 45° for a material that obeys the Tresca criterion, the observed direction of yield in PC is inclined at more than 45° to the tensile direction. This observation on the direction of the shear plane has been reported previously in polymers and is a result of the volume expansion that occurs during plastic yielding of PC and other glassy polymers [26].

Intersecting shear produces a necking effect in front of the notch as it opens. To accommodate the strain at the notch tip, the slip planes broaden so that the

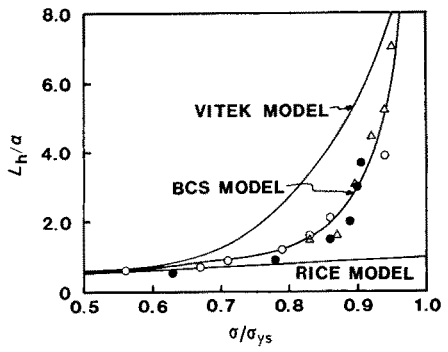

Figure 14 Length of hinge shear in 60° notch samples plotted against external load. Predictions from Vitek [21], BCS [23] and Rice [22] models are included for comparison. (●) 3.14 mm, (○) 4.70 mm, (△) 6.54 mm.

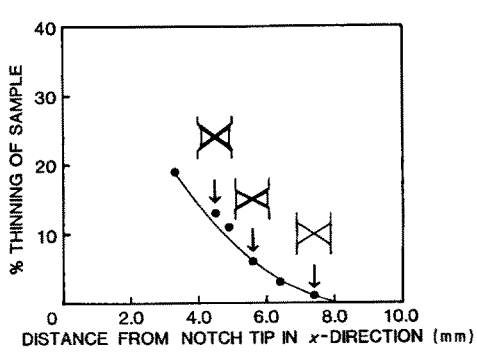

Figure 15 Per cent thinning in the yield zone of 1.20 mm thick PC with a semicircular notch plotted against distance from the notch tip.

TABLE I Predicted and observed transition from hinge shear to intersecting shear

Thickness (mm)	Hinge shear, below:		Intersecting shear, above:		Onset of hinge shear		Onset of intersecting shear	
	Stress* (MPa)	σ_{ys}†	Stress‡ (MPa)	σ_{ys}† (%)	Semicircular notch (MPa)	60° notch (MPa)	Semicircular notch (MPa)	60° notch (MPa)
1.20	43.4	70	55.2	89	37.4	35.7	45.8	43.6
3.14	52.4	85	59.1	95	42.6	42.0	55.2	53.0
4.70	55.0	89	60.0	97	45.5	44.0	58.7	59.0
6.54	56.7	91	60.5	98	56.8	52.0	–	–

*From Equation 4.
†Yield stress of unnotched polycarbonate, 62 MPa.
‡From Equation 5.

region between the slip planes becomes progressively thinner. Simultaneously the intersecting shear planes lengthen as more of the width reaches the yield stress. A damage zone that has progressed some distance across the width, such as that in Fig. 6c, shows the changes that occur in the neck profile. The neck profile at various distances from the notch tip is shown schematically in Fig. 15 together with the relative reduction in thickness. Broadening of the slip planes produces certain effects on the appearance of intersecting shear when viewed as in Fig. 6c including gradual broadening of the dark bands toward the notch and the increase in the overall dimension of the zone in the tensile direction

4.3. Transition from hinge shear to intersecting shear

The transition from plane strain hinge mode to plane stress intersecting shear apparently has only been reported in a study of edge-slotted silicon steel by Hahn and Rosenfield [18]. They discussed the conditions under which each mode should be dominant; with the assumption that intersecting shear is constrained until the yield stress is achieved a distance equal to half the sheet thickness above and below the crack plane, the condition for hinge shear dominance is

$$\frac{t}{a} > \sec\left(\frac{\pi\sigma}{2\sigma_{ys}}\right) - 1 \qquad (4)$$

where t is the sheet thickness. They also assumed that when the intersecting shear zone approaches a certain Dugdale-type shape, intersecting shear will predominate, specifically when

$$\frac{t}{a} < \frac{1}{4}\left[\sec\left(\frac{\pi\sigma}{2\sigma_{ys}}\right) - 1\right] \qquad (5)$$

Intermediate stresses constitute a transition region.

The onset stresses of hinge shear and intersecting shear were obtained from the series of micrographs which accompanied tensile loading experiments. The onset of hinge shear is taken as the first appearance of two dark regions above and below the notch tip. Because the onset of intersecting shear is more difficult to determine because of overlap with the hinge shear bands in the region near the notch, the stress at which the tips of parallel intersecting shear bands become visible is reported. The comparison in Table I shows that the experimental observations on semicircular and 60° notch specimens are consistent with the conditions suggested by Hahn and Rosenfield [18]. For each of the four thicknesses, only hinge shear is observed below the lower limit of the transition region given by Equation 4, while the onset of intersecting shear occurs at a stress within the transition region defined by Equations 4 and 5.

5. Conclusions

The modes of shear yielding before crack initiation in notched PC during slow tensile loading have been examined. By varying sheet thickness, conditions ranging from mostly plane strain to mostly plane stress were achieved. The study leads to the following conclusions.

1. Three shear yielding modes, namely core yielding, hinge shear and intersecting shear, are observed with increasing stress. Core yielding is observed in all thicknesses while hinge shear is predominant in thick sheet or the plane strain condition, and intersecting shear is predominant in thin sheet or the plane stress condition.

2. Core yielding consists of two families of shear flow lines contained in the centre region where the stress is highest. It cannot grow beyond a certain point due to constraints imposed by the surrounding elastic material.

3. Hinge shear initiates from the surface where a larger degree of freedom is available for extended yielding. Subsequently, it penetrates the entire thickness and grows above and below the core yielding at a particular angle related to the notch geometry. The dependence of hinge shear length on the applied tensile stress is described by the BCS model.

4. Intersecting shear is a result of a pair of shear flow lines that extend through the thickness of the specimen at an angle of 53° to the loading direction. It produces a necking effect in the yield zone.

5. The transition from hinge shear mode to intersecting shear mode follows the conditions suggested by Hahn and Rosenfield.

Acknowledgements

The authors thank Dr C. J. Chou, The Dow Chemical Company, Freeport, Texas, for providing the injection moulded samples. This work was generously supported by The Dow Chemical Company and the National Science Foundation (DMR 87-3041).

References

1. J. R. KASTELIC and E. BAER, *J. Macromol Sci. Phys.* **B7** (1973) 679.

2. N. J. MILLS, *J. Mater. Sci.* **11** (1976) 363.
3. M. KITAGAWA, *ibid.* **17** (1982) 2514.
4. M. ISHIKAWA, I. NARISAWA and H. OGAWA, *J. Polym. Sci. Polym. Phys. Edn* **15** (1977) 1791.
5. H. NISITANI and H. HYAKUTAKE, *Engng Fract. Mech.* **22** (1985) 359.
6. N. HADDAOUI, A. CHUDNOVSKY and A. MOET, *Polymer* **27** (1986) 1377.
7. N. J. MILLS and N. WALKER, *J. Mater. Sci.* **15** (1980) 1832.
8. M. T. TAKEMORI and R. P. KAMBOUR, *ibid.* **16** (1981) 1108.
9. M. T. TAKEMORI and D. S. MATSUMOTO, *J. Polym. Sci. Polym. Phys. Edn* **20** (1982) 2027.
10. H. F. BRINSON, *Exp. Mech.* **10** (1970) 72.
11. A. P. GREEN and B. B. HUNDY, *J. Mech. Phys. Solids* **4** (1956) 128.
12. G. LIANIS and H. FORD, *ibid.* **7** (1958) 1.
13. R. M. McMEEKING, *J. Engng Mater. Technol.* **99** (1977) 290.
14. R. HILL, "The Mathematical Theory of Plasticity" (Clarendon, Oxford, 1950).
15. E. OROWAN, in Proceedings of the International Conference on Physics, London 1934, Vol. 2 (University Press, Cambridge, 1935) p. 81.
16. A. H. COTTRELL, in "The Mechanical Properties of Matter" (Wiley, New York, 1964) p. 348.
17. F. J. P. CLARKE, R. A. SAMBELL and H. G. TATTERSALL, *Phil. Mag.* **7** (1962) 393.
18. G. T. HAHN and A. R. ROSENFIELD, *Acta Metall.* **13** (1965) 293.
19. T. R. WILSHAW and P. L. PRATT, *J. Mech. Phys. Solids* **14** (1966) 7.
20. B. A. BILBY and K. H. SWINDEN, *Proc. Roy. Soc. London A* **285** (1965) 22.
21. V. VITEK, *J. Mech. Phys. Solids* **24** (1976) 263.
22. J. R. RICE, *ibid.* **22** (1974) 17.
23. B. A. BILBY, A. H. COTTRELL and K. H. SWINDEN, *Proc. Roy. Soc. A* **272** (1963) 304.
24. A. S. TETELMAN, *Acta Metall.* **12** (1964) 993.
25. B. J. SCHAEFFER, H. W. LUI and J. S. KE, *Exp. Mech.* **11** (1971) 172.
26. W. WHITNEY and R. D. ANDREWS, *J. Polym. Sci. C* **16** (1967) 2981.

Received 1 September
and accepted 25 October 1988